Computer Chemistry

$[(\eta^6\text{-}B_6X)_2M]$ (X = C, N; M = Mn, Fe, Co, Ni): A New Class of Transition-Metal Sandwich-Type Complexes**

Si-Dian Li, Jin-Chang Guo, Chang-Qing Miao, and Guang-Ming Ren*

Metallocenes, including ferrocene, $[(\eta^5\text{-}C_5H_5)_2Fe]$, and its 18-electron analogues $[(\eta^5\text{-}E_5)_2M]$ (E = P, N, As, Sb, and Bi; M = transition-metal atom), have found important applications in both fundamental research and materials science.[1–8] Planar aromatic D_{6h} C_6H_6 and D_{4h} $[N_4]^{2-}$ and $[Al_4]^{2-}$ can also be utilized as ligands to coordinate transition metals and form similar $[(\eta^n\text{-}E_n)_2M]$ complexes ($n = 4, 6$).[9–11] In these sandwich-type structures, the transition-metal center, M, is coordinated between two aromatic η^n-E_n monocycles ($n = 4$–6), each of which has 6-π electrons. The π–d interactions between the delocalized π molecular orbitals (MOs) of the ligands and the partially occupied d orbitals of the transition-metal center play a crucial role in stabilizing the systems. Designing new forms of metallocenes and their sandwich-type analogues requires the right match between the monocyclic ligands and transition-metal centers, both geometrically and electronically. Inspired by the proposed 6-π electron aromatic D_{6h} B_6C^{2-} ion featuring a carbon atom in a planar hexacoordinate environment (denoted phC) at the center of a perfect B_6 hexagon,[12] we present herein an investigation by density functional theory (DFT) of a new class of sandwich-type complexes, D_{6d} $[(\eta^6\text{-}B_6X)_2M]$ (X = C, N; M = Mn, Fe, Co, Ni). These complexes are unique in that they contain two parallel η^6-B_6X hexagons centered with two nearly planar hexacoordinate carbon or nitrogen atoms (phN) located along the sixfold molecular axis. The results obtained in this work provide an important extension to the traditional concept of sandwich-type complexes by incorporating hexacoordinate carbon or nitrogen atoms in the systems and present a viable possibility to stabilize and characterize phC or phN atoms in future experiments. To the best of our knowledge, there have been no investigations reported to date on B_6C^{2-} ligands in metallocene-like complexes.

[*] Prof. S.-D. Li, Dr. J.-C. Guo, C.-Q. Miao, G.-M. Ren
Institute of Materials Sciences and
Department of Chemistry
Xinzhou Teachers' University
Xinzhou 034000, Shanxi (P. R. China)
and
Institute of Molecular Science
Shanxi University
Taiyuan 030001, Shanxi (P. R. China)
Fax: (+86) 350-303-1845
E-mail: lisidian@yahoo.com

[**] This work was financially supported by the Shanxi Natural Science Foundation. The authors thank Dr. Hai-Jun Jiao for inspiring discussions.

Supporting information for this article is available on the WWW under http://www.angewandte.org or from the author.

DFT structural optimizations at the B3LYP/6-311 + G(3df) level[13–15] were performed on the sandwich complexes under investigation and imaginary frequencies and DFT wavefunction instabilities checked at the same theoretical level. Natural bond orbital (NBO)[16] analyses were implemented to gain insight into the bonding pattern of the complexes. Figure 1 and Figure 2 depict the optimized

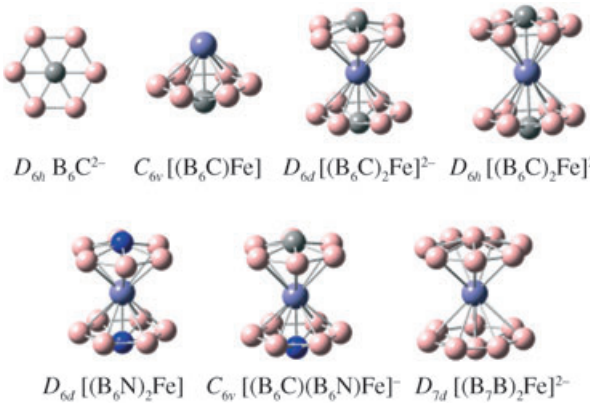

Figure 1. Optimized structures of D_{6h} B_6C^{2-}, C_{6v} $[(B_6C)Fe]$, D_{6d} $[(B_6C)_2Fe]^{2-}$, D_{6h} $[(B_6C)_2Fe]^{2-}$, D_{6d} $[(B_6N)_2Fe]$, C_{6v} $[(B_6C)(B_6N)Fe]^-$, and D_{7d} $[(B_7C)_2Fe]^{2-}$.

structures of Fe-containing complexes, and Figure 3 shows the MO pictures of the top 13 occupied energy levels of D_{6d} $[(\eta^6\text{-}B_6C)_2Fe]^{2-}$ (with one orbital shown for two degenerate MOs). These optimum structures are well-maintained when symmetry constraints are removed. Co-, Ni-, and Mn-centered complexes have the same geometries and similar MOs but have different energy levels. Table 1 tabulates the calculated bond lengths, natural atomic charges, lowest vibrational frequencies ($\tilde{\nu}_{min}$), highest occupied molecular orbital (HOMO) energies, and total Wiberg bond indices (WBIs)[12,17] of the constituent atoms for the complexes under investigation. Detailed geometrical and electronic properties of 28 neutral and charged complex ions that contain B_6X^{2-} (X = C, N) and B_7B^{2-} ligands are tabulated in the Supporting Information. All the calculations in this work were carried out by using the Gaussian 03 program.[17]

When a transition-metal center M (M = Mn, Fe, Co) coordinates one η^6-B_6C^{2-} ligand along the sixfold axis, a hexagonal-bipyramidal C_{6v} $[(\eta^6\text{-}B_6C)M]$ complex is formed (see Figure 1). The 12-electron C_{6v} $[(\eta^6\text{-}B_6C)Mn]^-$, $[(\eta^6\text{-}B_6C)Fe]$, and $[(\eta^6\text{-}B_6C)Co]^+$ species are all found to be true minima with the lowest vibrational frequencies greater than 280 cm^{-1}. Adding one more η^6-B_6C^{2-} ligand to a C_{6v} $[(\eta^6\text{-}B_6C)M]$ complex from the opposite direction along the sixfold axis results in a staggered D_{6d} $[(\eta^6\text{-}B_6C)_2M]$ complex, which contains two parallel C_{6v} B_6C^{2-} ligands around the transition-metal center. D_{6d} $[(\eta^6\text{-}B_6C)_2M]$ complexes have practically the same B–B bond lengths as C_{6v} $[(B_6C)M]$ but have slightly shorter B–C bonds and longer B–Fe separations as indicated in Table 1. The DFT Fe–B bond lengths in D_{6d} $[(\eta^6\text{-}B_6C)_2Fe]^{2-}$ are about 0.194 Å longer than the Fe–C separation (2.064 Å) observed in $[(\eta^5\text{-}C_5H_5)_2Fe]$.[9] The C atoms in D_{6d} $[(\eta^6$-

  DOI: 10.1002/ange.200462476

Table 1: Optimized bond lengths, r [Å]; natural atomic charges, q [$|e|$]; lowest vibrational frequencies, $\tilde{\nu}_{min}$ [cm^{-1}]; HOMO energies [eV]; total Wiberg bond indices (WBIs) of the constituent atoms of D_{6h} B_6C^{2-}, D_{6h} B_6N^-, and D_{7h} B_7B^{2-} ligands and their sandwich complexes.

	r_{B-B}	r_{B-X}	r_{B-M}	r_{X-M}	q_B	q_X	q_M	$\tilde{\nu}_{min}$	WBI_B	WBI_X	WBI_M	HOMO
D_{6h} B_6C^{2-}	1.588	1.588			−0.21	−0.76		270	3.65	3.84		+4.18
C_{6v} $[Li(B_6C)]^-$	1.579	1.594	2.360	1.968	−0.19	−0.78	+0.92	291	3.64	3.87	0.02	−0.67
C_{6v} $[(B_6C)Mn]^-$	1.579	1.676	2.100	1.946	−0.12	−0.56	+0.31	312	3.63	3.93	3.67	+0.09
C_{6v} $[(B_6C)Fe]$	1.570	1.660	2.108	1.947	+0.02	−0.59	+0.48	282	3.53	3.93	3.21	−5.09
C_{6v} $[(B_6C)Co]^+$	1.574	1.665	2.135	1.982	+0.17	−0.67	+0.67	309	3.38	3.90	2.63	−12.40
D_{6d} $[(B_6C)_2Fe]^{2-}$	1.578	1.626	2.258	2.003	−0.01	−0.74	−0.42	43	3.54	3.86	3.03	+2.09
D_{6d} $[(B_6C)_2Co]^-$	1.580	1.619	2.265	1.974	+0.05	−0.79	+0.03	45	3.50	3.86	2.38	−2.46
D_{6d} $[(B_6C)_2Ni]$	1.588	1.616	2.302	1.964	+0.11	−0.89	+0.51	39	3.44	3.83	1.70	−6.75
D_{6h} B_6N^-	1.579	1.579			−0.02	−0.91		282i	3.45	3.17		−0.41
D_{6d} $[(B_6N)_2Fe]$	1.594	1.648	2.205	1.942	+0.20	−0.99	−0.40	58	3.30	3.06	3.11	−6.65
C_{6v} $[(B_6C)(B_6N)Fe]^-$	N 1.594	1.672	2.141	1.935	+0.13	−0.96	−0.38	55	3.35	3.05	3.17	−2.29
	C 1.578	1.617	2.300	2.026	+0.05	−0.76			3.49	3.86		
D_{6d} $[(B_6N)_2Mn]^-$	1.593	1.673	2.190	2.015	+0.14	−0.96	−0.78	63	3.34	3.05	3.69	−1.58
D_{7h} B_7B^{2-}	1.546	1.781			−0.30	+0.08		328	3.77	3.73		+3.44
D_{7d} $[(B_7B)_2Fe]^{2-}$	1.533	1.814	2.419	2.067	−0.12	−0.04	−0.427	37	3.68	3.76	2.98	+1.55
D_{7d} $[(B_7B)_2Co]^-$	1.534	1.813	2.408	2.040	−0.07	−0.004	−0.01	39	3.63	3.78	2.38	−2.91
D_{7d} $(B_7B)Ni$	1.542	1.815	2.427	2.027	−0.018	−0.101	+0.45	37	3.58	3.84	1.68	−6.98

$B_6C)_2Fe]^{2-}$, $[(\eta^6\text{-}B_6C)_2Co]^-$, and $[(\eta^6\text{-}B_6C)_2Ni]$ are only 0.39, 0.35, and 0.30 Å above the B_6 planes and can be approximately treated as quasi-phC atoms.

Although the energy differences between the staggered (D_{6d}) and the eclipsed (D_{6h}) conformations are very small and both structures have similar MOs, the eclipsed $[(\eta^6\text{-}B_6C)_2M]$ complexes all turn out to be transition states with one imaginary frequency. For example, for $[(\eta^6\text{-}B_6C)_2Fe]^{2-}$, $[(\eta^6\text{-}B_6C)_2Co]^-$, and $[(\eta^6\text{-}B_6C)_2Ni]$, the calculated energy differences between the eclipsed and staggered conformations are only 2.80, 2.88, and 2.41 kJ mol^{-1}, respectively, and their eclipsed structures are found to have one imaginary vibrational frequency located at 38i (b_{2g}), 39i (a_{1u}), and 32i (b_{2g}) cm^{-1}, respectively. This situation is different from the eclipsed D_{5h} $[(\eta^5\text{-}C_5H_5)_2Fe]$ observed in the gas phase[9] and D_{5h} $[(\eta^5\text{-}P_5)_2Ti]^{2-}$ in solids.[5] As the transition states are on rotational paths, the eclipsed D_{6h} $[(\eta^6\text{-}B_6C)_2M]$ complexes are automatically transferred to the staggered conformation when relaxed in the modes with the imaginary frequencies mentioned above. Thus, the complexes have very low rotational-energy barriers between D_{6d} and D_{6h} $[(\eta^6\text{-}B_6C)_2M]$, which is similar to the situation for D_5 ferrocene[9] (a slight distortion from a perfect D_{5h} $[(\eta^5\text{-}C_5H_5)_2Fe]$ as revealed by DFT). The contribution of the transition-metal centers in stabilizing these sandwich complexes is best illustrated in the cases of D_{6d} $[(\eta^6\text{-}B_6N)_2Fe]$, C_{6v} $[(\eta^6\text{-}B_6C)(\eta^6\text{-}B_6N)Fe]^-$, and D_{6d} $[(\eta^6\text{-}B_6N)_2Mn]^-$, in which the unstable phN centers in D_{6h} B_6N^- (which has an imaginary frequency at 282i cm^{-1} in e_{1u} mode) have been stabilized when incorporated in sandwich complexes. As indicated in Figure 1 and Table 1, the sandwich-type D_{7d} $[(\eta^7\text{-}B_7B)_2M]$ complexes (M = Fe, Co, Ni), which contain two 6-π-electron heptagons (D_{7h} B_7B^{2-}) centered with two B atoms,[18] are also true minima of the systems.

It is interesting to study reaction (1) of D_{6h} B_6C^{2-} with D_5 $[(C_5H_5)_2Fe]$ to produce D_{6d} $[(B_6C)_2Fe]^{2-}$ and D_{5h} $C_5H_5^-$. With zero-point corrections included, the reaction (1) is highly exothermic as calculated by DFT and has an enthalpy change of $\Delta H^0 = -530.9$ kJ mol^{-1} and a Gibbs free energy change of $\Delta G^0 = -533.6$ kJ mol^{-1}, which indicates that the replacement of $C_5H_5^-$ in D_5 $[(\eta^5\text{-}C_5H_5)_2Fe]$ with B_6C^{2-} is strongly favored thermodynamically. Based upon this observation, we propose to synthesize stable and characterizable salts of $[(B_6C)_2Fe]^{2-}$ containing phC atoms as outlined in Equation (1). Further investigation on the reaction kinetics is currently in progress.

$$[(C_5H_5)_2Fe] + 2\,B_6C^{2-} \rightarrow [(B_6C)_2Fe]^{2-} + 2\,C_5H_5^- \quad (1)$$

Why are these sandwich-type structures stable? NBO analyses help to answer this question. D_{6d} $[(B_6C)_2Fe]^{2-}$ has the natural atomic electronic configurations of C, $[He]2s^{1.04}2p^{3.60}$ $(2s^{1.04}2p_x^{1.27}2p_y^{1.27}2p_z^{1.05})$; Fe, $[Ar]4s^{0.16}3d^{8.18}$ $(4s^{0.16}3d_{xy}^{1.88}3d_{xz}^{1.38}3d_{yz}^{1.38}3d_{x^2-y^2}^{1.88}3d_{z^2}^{1.66})$; and B, $[He]2s^{0.86}2p^{2.12}$ $(2s^{0.86}2p_x^{0.99}2p_y^{0.55}2p_z^{0.58})$, which are in agreement with the natural atomic charges tabulated in Table 1. The $4s^2$ electrons of the neutral Fe have been almost completely stripped away in $[(B_6C)_2Fe]^{2-}$, with the occupancy of the 4s orbital of the Fe atom decreased to $4s^{0.16}$. The negative charge of the Fe atom (−0.42 $|e|$) results from the π→d back-bonding from the B_6C^{2-} ligands to the Fe center. Similar to the situation in D_{6h} B_6C^{2-}, a C center provides three sp^2-hybridized orbitals to form six partial bonds with the surrounding B atoms and provides one singly occupied p_z orbital to participate in the formation of the delocalized MOs within the complex (HOMO-9 and HOMO-12 shown in Figure 2). The electron-deficient peripheral B atoms each

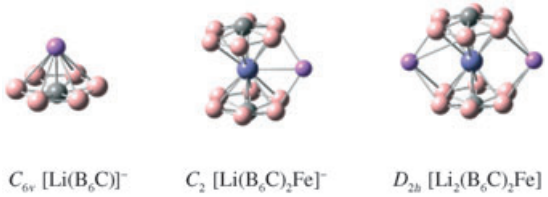

Figure 2. Optimized structures of C_{6v} $[LiB_6C]^-$, C_2 $Li[(B_6C)_2Fe]^-$, and D_{2h} $Li_2[(B_6C)_2Fe]$.

contribute three partially occupied sp^2-hybridized orbitals to form three in-plane bonds and provide one partially filled p_z orbital to participate in the π–d interaction with the metal center.

Orbital analyses indicate that all the occupied MOs of $[(B_6C)_2Fe]^{2-}$ can be unambiguously assigned to different combinations of the frontier MOs of the two D_{6h} B_6C^{2-} ligands and the 3d orbitals of the Fe center (Figure 3). The

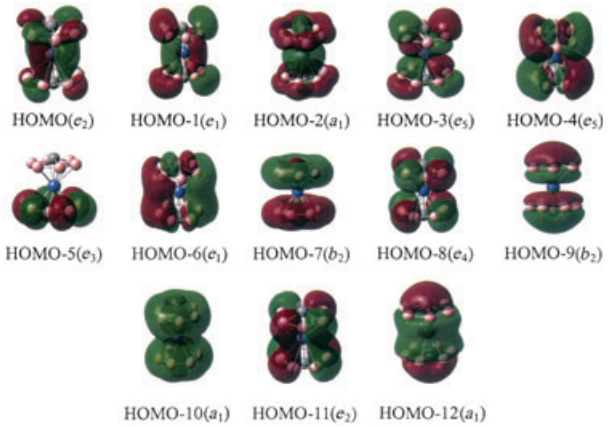

Figure 3. Molecular orbital pictures of the top 13 energy levels of D_{6d} $[(B_6C)_2Fe]^{2-}$.

degenerate HOMOs (e_2) originate from the nearly fully occupied Fe $3d_{xy}^{1.88}$ and Fe $3d_{x^2-y^2}^{1.88}$ orbitals. The degenerate HOMO-1(e_1) mainly represent the in-phase overlaps between the two delocalized π HOMOs (e_{1g}) of the two B_6C^{2-} ligands,[12] whereas HOMO-3(e_5) reflects the interactions between the two π HOMOs (e_{1g}) of the two B_6C^{2-} ligands with opposite orbital signs and the $3d_{xz}^{1.38}$ and $3d_{yz}^{1.38}$ orbitals of the Fe center, which match the ligands in orbital signs and geometries. Interestingly, it is mainly the in-phase participation of the Fe 3d orbitals in HOMO-3(e_5) that makes the two degenerate HOMO-3(e_5) MOs lie lower in energy than HOMO-1(e_1). HOMO-2(a_1) and HOMO-10(a_1), which form the weak Fe–C interactions (as indicated by the Wiberg bond index detailed below) along the sixfold axis, mainly correspond to out-of-phase and in-phase overlaps of Fe $3d_{z^2}$ and C 2s orbitals, respectively. HOMO-4(e_5) and HOMO-6(e_1) clearly originate from the four degenerate HOMO-1(e_{1u}) orbitals of the two B_6C^{2-} ligands. HOMO-5(e_3) and HOMO-7(b_2) are directly inherited from the HOMO-2(b_{2u}) and HOMO-3(a_{1g}) of the B_6C^{2-} ion, while HOMO-8(e_4) and HOMO-11(e_2) result from different combinations of the degenerate HOMO-4(e_{2g}) of the two ligands. Finally, HOMO-9(b_2) and HOMO-12(a_1) correspond to the out-of-phase and in-phase combinations of the two totally delocalized π HOMO-5(a_{2u}) of the two ligands, respectively.

The calculated total Wiberg bond indices (WBIs) of the constituent atoms with $WBI_C = 3.83–3.93$, $WBI_N = 3.05–3.17$, $WBI_B = 3.30–3.68$, and $WBI_M = 1.68–3.69$ indicate that these complexes follow the octet role in bonding nature, similar to the situation observed in the D_{6h} B_6C^{2-} ion.[12] The introduction of a transition-metal center, M, leads to two additional C–M interactions and twelve additional B–M interactions, whereas the C–B and B–B bonds in B_6C^{2-} ligands are well maintained. For example, the Wiberg bond orders of D_{6d} $[(B_6C)_2Fe]^{2-}$ are $WBI_{C-B} = 0.60$, $WBI_{B-B} = 1.17$, $WBI_{Fe-C} = 0.19$, and $WBI_{Fe-B} = 0.22$, of which, WBI_{C-B} and WBI_{B-B} are practically the same as the corresponding values of 0.64 and 1.26 in a perfect D_{6h} B_6C^{2-} hexagon calculated at the same DFT level.

It should be pointed out that, as expected, D_{6d} $[(\eta^6\text{-}B_6C)_2Fe]^{2-}$ is unstable towards electron dissociation: its top nine occupied MOs have positive eigenvalues when calculated by DFT. Similar situations are met in other dianions such as D_{6h} B_6C^{2-}[12] and D_{4h} $[Al_4]^{2-}$ and D_{4d} $[Al_4TiAl_4]^{2-}$,[11] all of which have positive HOMO energies. However, these aromatic dianions can be effectively stabilized by introducing alkali-metal counterions into the systems while keeping the basic structures of the dianions unchanged, as shown in the cases of C_{4v} $[MAl_4]^-$ (M = Li, Na, Cu) and $[NaAl_4TiAl_4]^-$.[11] C_{6v} $[LiB_6C]^-$, C_2 $[Li(\eta^6\text{-}B_6C)_2Fe]^-$, and D_{2h} $[Li_2(\eta^6\text{-}B_6C)_2Fe]$ studied in this work (see Figure 2) are confirmed to have the negative HOMO energies of −0.67, −1.82 ,and −5.68 eV, respectively. The structures of B_6C^{2-} ligands are well maintained in these complexes and the staggered→eclipsed structural change is completed in D_{2h} $[Li_2(\eta^6\text{-}B_6C)_2Fe]$, in which the relatively strong Coulomb attractions between the two Li^+ ions and their neighboring B atoms with partial negative charges determine the structure of the neutral complex. All the occupied MOs of other neutral and monoanionic sandwich complexes tabulated in Table 1 are confirmed to have negative energies. According to Koopman's theorem, the negative values of the HOMO energies listed in Table 1 approximately represent the first-electron-detachment energies of the corresponding complexes.

In summary, we have predicted by DFT a new class of sandwich-type complexes D_{6d} $[(B_6X)_2M]$ with two nearly planar hexacoordinate carbon or nitrogen atoms located at the centers of two parallel B_6 hexagons about the transition-metal center M. The proposal of replacing C_5H_5- in $[(\eta^5\text{-}C_5H_5)_2Fe]$ with B_6C^{2-} to form D_{6d} $[(\eta^6\text{-}B_6C)_2Fe]^{2-}$ may represent a step forward towards the synthesis and characterization of phC centers incorporated in transition-metal complex salts in future experiments. The sandwich structural pattern developed in this work may be extended along the sixfold molecular axis (or in its perpendicular direction) to form $[(B_6C)M]_n$ chains ($n \geq 3$) linked with alkali-metal cations and the hexagonal B_6 centered with C or N may be modified to form various heterocyclic ligands.

Received: October 30, 2004
Revised: December 17, 2004
Published online: March 2, 2005

Keywords: boron · computer chemistry · density functional calculations · electronic structures · hexacoordinate carbon

[1] T. J. Kealy, P. L. Pauson, *Nature* **1951**, *168*, 1039.
[2] N. J. Long, *Metallocenes*, Blackwell, Oxford, UK, **1998**.
[3] A. D. Garnovskii, A. P. Sadimenko, M. I. Sadimenko, D. A. Garnovskii, *Coord. Chem. Rev.* **1998**, *173*, 31.

[4] P. v. R. Schleyer, B. Kiran, D. V. Simion, T. S. Sorensen, *J. Am. Chem. Soc.* **2000**, *122*, 510.
[5] E. Urnezius, W. W. Brennessel, C. J. Cramer, J. E. Ellis, P. v. R. Schleyer, *Science* **2002**, *295*, 832.
[6] A. C. Tsipis, A. T. Chaviara, *Inorg. Chem.* **2004**, *43*, 1273.
[7] M. Lein, J. Frunzke, G. Frenking, *Angew. Chem.* **2003**, *115*, 1341; *Angew. Chem. Int. Ed.* **2003**, *42*, 1303.
[8] M. Lein, J. Frunzke, A. Timoshkin, G. Frenking, *Chem. Eur. J.* **2001**, *7*, 4155.
[9] A. Haaland, *Acc. Chem. Res.* **1979**, *12*, 415.
[10] J. M. Mercero, J. M. Matxain, J. M. Ugalde, *Angew. Chem.* **2004**, *116*, 5601; *Angew. Chem. Int. Ed.* **2004**, *43*, 5485.
[11] X. Li, A. E. Kuznetsov, H. F. Zhang, A. I. Boldyrev, L.-S. Wang, *Science* **2001**, *291*, 859; J. M. Mercero, J. M. Ugalde, *J. Am. Chem. Soc.* **2004**, *126*, 3380.
[12] K. Exner, P. v. R. Schleyer, *Science* **2000**, *290*, 1937.
[13] A. D. Becke, *J. Chem. Phys.* **1993**, *98*, 5648.
[14] C. Lee, W. Yang, R. G. Parr, *Phys. Rev. B* **1988**, *37*, 785.
[15] S. H. Vosko, L. Wilk, M. Nusair, *Can. J. Phys.* **1980**, *58*, 1200.
[16] J. E. Carpenter, F. Weinhold, *J. Mol. Struct.* **1988**, *169*, 41.
[17] Gaussian 03 (Revision A.1), M. J. Frisch, G. W. Trucks, H. B. Schlegel, G. E. Scuseria, M. A. Robb, J. R. Cheeseman, J. A. Montgomery, Jr., T. Vreven, K. N. Kudin, J. C. Burant, J. M. Millam, S. S. Iyengar, J. Tomasi, V. Barone, B. Mennucci, M. Cossi, G. Scalmani, N. Rega, G. A. Petersson, H. Nakatsuji, M. Hada, M. Ehara, K. Toyota, R. Fukuda, J. Hasegawa, M. Ishida, T. Nakajima, Y. Honda, O. Kitao, H. Nakai, M. Klene, X. Li, J. E. Knox, H. P. Hratchian, J. B. Cross, C. Adamo, J. Jaramillo, R. Gomperts, R. E. Stratmann, O. Yazyev, A. J. Austin, R. Cammi, C. Pomelli, J. W. Ochterski, P. Y. Ayala, K. Morokuma, G. A. Voth, P. Salvador, J. J. Dannenberg, V. G. Zakrzewski, S. Dapprich, A. D. Daniels, M. C. Strain, O. Farkas, D. K. Malick, A. D. Rabuck, K. Raghavachari, J. B. Foresman, J. V. Ortiz, Q. Cui, A. G. Baboul, S. Clifford, J. Cioslowski, B. B. Stefanov, G. Liu, A. Liashenko, P. Piskorz, I. Komaromi, R. L. Martin, D. J. Fox, T. Keith, M. A. Al-Laham, C. Y. Peng, A. Nanayakkara, M. Challacombe, P. M. W. Gill, B. Johnson, W. Chen, M. W. Wong, C. Gonzalez, J. A. Pople, Gaussian, Inc., Pittsburgh, PA, **2003**..
[18] H. J. Zhai, A. N. Alexandrova, K. A. Birch, A. I. Boldyrev, L. S. Wang, *Angew. Chem.* **2003**, *115*, 6186; *Angew. Chem. Int. Ed.* **2003**, *42*, 6004.

